

An L-Band Bandpass Filter with Narrow Bandwidth and Miniature Based on LTCC Technology

Cheng Tan^{1, 2, *}, Zhongjun Yu¹, and Chunshuang Xie^{1, 2}

Abstract—In this paper, in order to meet the requirements for miniaturizing a microwave frequency conversion module, an L-band filter with narrow band and high out-of-band rejection is designed based on LTCC technology. The values of each element in the simplified schematic diagram are used with Chebyshev type function being the prototype, and the shapes and layout of the elements are reasonably designed for effectively utilizing the electromagnetic coupling effect inside the structure. The actually processed filter has a bandwidth of 20 MHz, and its out-of-band rejection reaches 39 dB and 42 dB at 1 GHz and 1.6 GHz, respectively.

1. INTRODUCTION

As an important part of a high frequency circuit, filter is often used to select signals within a specific frequency band, and at the same time, it has certain rejection on the out-of-band spurious frequency. The lumped parameter LC filter is a common type of filter [1–4]. LC filters are mostly arranged by capacitors, inductors, and resistors according to the design method, so that they have frequency selectivity to the signals. However, due to its composition and structure, the development of LC filters has been restrained. The package dimensions of the components which comprise filters are relatively large and not easy to be reduced.

Many existing literatures describe the methods for miniaturizing a filter, such as hairpin resonant unit [5], folded stripline resonant unit [6], and spiral resonant unit [7]. These theories and methods have greatly reduced the size of a resonant unit to 1/4 wavelength or even 1/8 wavelength [8]. However, the application of these theories and methods in L-band cannot effectively reduce the size of the resonant element. Taking advantage of the LTCC technology in a three-dimensional structure, lump-capacitor inductance is realized in the Z direction by means of stacking [9], thus the volume of the filter can be effectively reduced, and the integrity and reliability of the LC filter are improved. Miniaturized LTCC LC filter has pushed the rapid development of civil and military electronic products in the direction of high reliability, miniaturization, high performance, and low cost.

Low Temperature Co-fired ceramic (LTCC) technology is a multi-layer ceramic technology [10–13]. LTCC is featured with three-dimensional wiring [14]. Meanwhile, passive components can be embedded into the interior of multi-layer ceramics, so that the miniaturization and integration of passive devices and circuits can be realized. Based on the LTCC multi-layer technology, capacitor is realized through the stacked structure, and inductor is realized through the form of the spiral coupling line. Then, the vertical interconnection of LTCC wires is utilized, thus completing the design of the filter. The LTCC technology makes filter design more compact. Thus the stability of the filter is improved, and the size of the filter is greatly reduced.

Received 9 September 2019, Accepted 19 November 2019, Scheduled 4 December 2019

* Corresponding author: Tan Cheng (tancheng1102@163.com).

¹ Aerospace Information Research Institute, Chinese Academy of Sciences, Beijing, P. R. China. ² School of Electronic, Electrical and Communication Engineering, University of Chinese Academy of Sciences, Beijing, P. R. China.

The filter designed in this paper is a narrow-band filter which has a bandwidth of 20 MHz and requires high out-of-band rejection. A traditional filter is usually implemented by a crystal filter or a SAW filter, but it cannot meet the system requirements due to its large size. In this paper, a bandpass filter with a small size, narrow bandwidth and high out-of-band rejection is designed on the basis of LTCC technology. Transmission zeros are introduced into the LC filter model, and a filter with narrow-band and high out-of-band rejection is obtained by reasonable transformation of the structure. Its volume is only $5 \text{ mm} \times 4.1 \text{ mm} \times 1.0 \text{ mm}$.

2. DESIGN OF THE FILTER

At the time making the LC filter by means of the LTCC process, the circuit is implemented by making the capacitors and inductors with conductive materials respectively and embedding them in the LTCC medium [15]. All the components are fabricated with Ferro A6M material from Ferro company, which has a dielectric constant of 5.9 and a tangential value of loss angle of 0.002. The specific performance requirements of the designed bandpass filters are as shown in Table 1.

Table 1. Estimated indicators of the filter.

| Item | Feature |
|-----------------------|--|
| Passband range | 1.265 ~ 1.285 GHz |
| Insertion loss | $\leq 2 \text{ dB}$ |
| Out-of-band rejection | $\geq 35 \text{ dBc@1 GHz}$ $\geq 35 \text{ dBc@1.6 GHz}$ |
| VSWR | ≤ 1.5 |
| Dimensions | 5 mm \times 4.1 mm \times 1.0 mm |

2.1. Principle of the Filter

From the indicators in Table 1, it can be found that the out-of-band rejection requirement of the filter is relatively high. In the design of the filter, there are two ways to increase the out-of-band rejection of the filter. One is to increase the order of the filter, and the other is to add transmission zeros into the filter. It is true that its out-of-band rejection can be increased by increasing the order of the filter. However, with the increase of the order, the size of the filter will also increase, which is not conducive to the design of the miniaturized filter. As a result, the method of adding the transmission zeros is usually used in the design of the miniaturized filter [16, 17].

The zero point of the filter is the point where the transmission equation is equal to zero. In an ideal situation, the energy cannot pass at this frequency at all, so a good isolation effect could be achieved. In lumped parameter mode, the method of introducing series or parallel resonance is usually adopted in adding of the transmission zero into the filter. The schematic diagram is as shown in Figure 1.

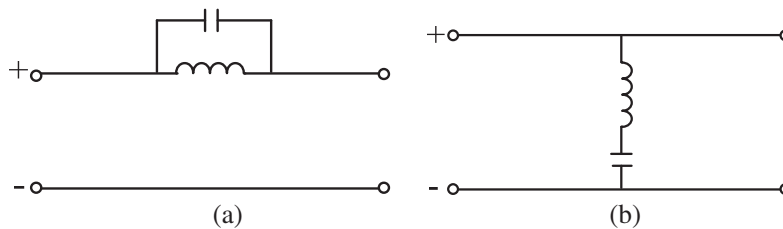


Figure 1. (a) The parallel resonance circuit. (b) The series resonance circuit.

The calculation formulas of the impedance and admittance in the high-frequency circuit when the capacitors and inductors in the circuit are installed in series or installed in parallel are as follows:

$$jB(\omega) = j\omega L + \frac{1}{j\omega C} \tag{1}$$

$$jX(\omega) = j\omega L \frac{1}{j\omega C} \tag{2}$$

Refer to Eq. (1), when LC meets the resonance relationship, the input impedance in the series resonance circuit is zero, and the circuit is equivalent to a short circuit. All the energy at this frequency is absorbed, and the transmission zero is formed. Referring to Eq. (2), when the admittance in the parallel resonance circuit is zero, the circuit is equivalent to an open circuit; the energy at this frequency is fully reflected; and the transmission zero point is formed.

2.2. The Prototype of the Bandpass Filter Circuit

On the basis of Chebyshev function, two transmission zeros are introduced into the filter. Modifications are made to Chebyshev type so that the sideband rejection is enhanced. The design of the filter equivalent schematic diagram is accomplished by means of Ansoft Designer software, as shown in Figure 2. Design equations for calculating the element values of the proposed filter structures can be derived by using the standard filter synthesis procedures [18].

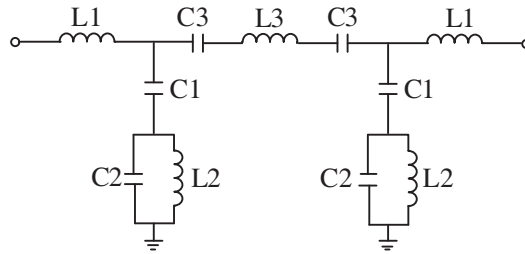


Figure 2. Ansoft Designer simulation circuit.

For the particular circuits shown in Figure 2, the component values are simply given by

$$C1 = \frac{1}{L2} \left(\frac{1}{\omega_z^2} - \frac{1}{\omega_p^2} \right) \tag{3a}$$

$$C2 = \frac{1}{\omega_p^2 L2} \tag{3b}$$

$$C3 = \frac{C_S}{\sqrt{2}} \cdot \frac{BW}{\omega_0} \tag{3c}$$

$$L2 = \frac{1}{C_{eff}} \cdot \frac{\omega_z^2 - \omega_p^2}{\omega_p^4} \cdot \frac{\omega_0^2 - \omega_p^2}{\omega_0^2 - \omega_z^2} \tag{3d}$$

where

$$\omega_p = \frac{(1 - k)\omega_0^4 + (k - 3)\omega_0^2\omega_z^2}{(k - 1)\omega_z^2 - (k + 1)\omega_0^2}$$

$$k = \frac{-2C_S}{C_{eff}}$$

$$C_{eff} = C3 - \omega_0 C3 Z_0$$

ω_0 and ω_z are the passband center frequency and transmission zero frequency, respectively. BW is the 1 dB bandwidth, and C_S is the shunt capacitors of the resonators associated with the standard filter design. $L1$ and $L3$ are just the connecting line, and the values are very small. The floating values of

$L1$ and $L3$ so not affect the results very much, so we could estimate the valuea. After calculation, the initial value of the circuit model is extracted as, $C1 = 0.96$ pF, $C2 = 5$ pF, $C3 = 0.81$ pF, $L1 = 0.26$ nH, $L2 = 1.82$ nH, $L3 = 0.32$ nH.

Since the required filter is a narrow-band filter, any minor adjustments to the capacitor value and inductor value are likely to affect the bandwidth of the filter. In the process of final implementation of the filter with the LTCC technology, the phenomenon of mutual coupling surely exists. Therefore, simulation in HFSS software is very important in this work. In Ansoft Designer software, the simulation result is as shown in Figure 3.

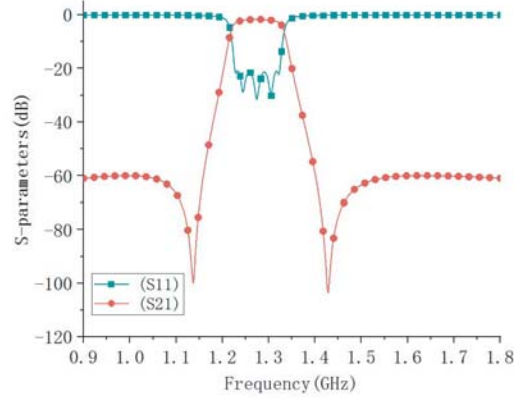


Figure 3. Results of the lumped circuit simulation with Ansoft Designer software.

3. SETTING UP OF THE MODEL

3.1. Three-Dimensional Model for the Inductor

LTCC inductors generally contain plane type and spiral type. The inductor values of $L1$ and $L3$ in the filter model are small, which is realized by a short line. The width of the inductor is 0.2 mm, which is the width of the $50\ \Omega$ stripline. The length of the inductor is obtained through HFSS simulation. The lengths of $L1$, $L2$, and $L3$ are 0.82 mm, 1.2 mm, and 4.4 mm, respectively. Inductor $L2$ is the key inductor in the filter, which involves the generation of transmission zero point. In order to avoid the mutual coupling with other capacitors, the plane type inductor is adopted. The inductor with this kind of structure has a high self-resonance frequency and quality factor.

The effective inductor value of LTCC can be expressed with the scattering parameter as follows:

$$L_{eff} = -\frac{1}{2\pi f \times im(Y_{11})} \quad (4)$$

where L_{eff} is the effective value of the inductor, f the self-resonant frequency, and Y_{11} the admittance value of the inductor. The three-dimensional model for the inductor with an inductance value of 1.82 nH is as shown in Figure 4. The conductor width in the inductor is 0.2 mm; the length in the direction of X axis is 2.9 mm; and the length in the direction of Y axis is 1.5 mm. The effective inductance value obtained by HFSS software simulation is as shown in Figure 5.

3.2. Three-Dimensional Model for the Capacitor

Capacitor is a main component in implementation of a filter circuit. For capacitors in the LTCC technology, mainly two kinds of structures are adopted, Metal-Insulator-Metal (MIM) structure and Vertically interdigitated Capacitor (VIC) structure. The commonly used structures are as shown in Figure 6.

With the same capacitor values being realized, MIM structure capacitor has a larger area and fewer occupied layers, while VIC structure capacitor has more advantages with respect to the Q value and

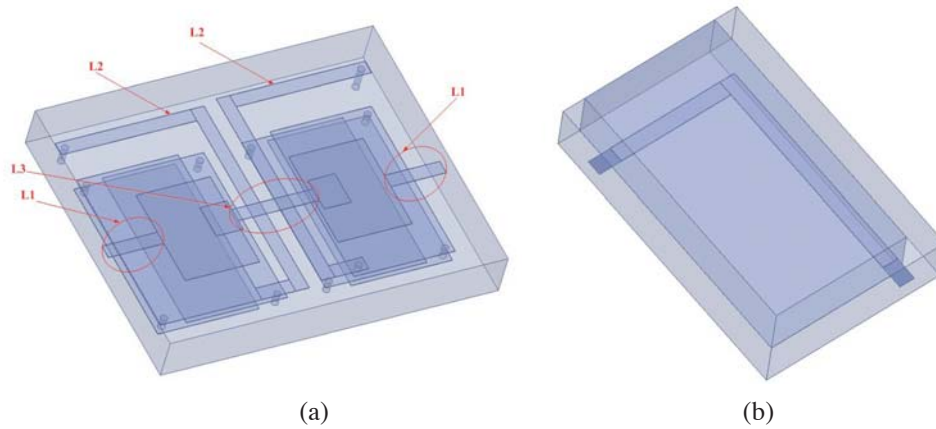


Figure 4. (a) Indicator of LTCC inductors. (b) A three-dimensional model of $L2$.

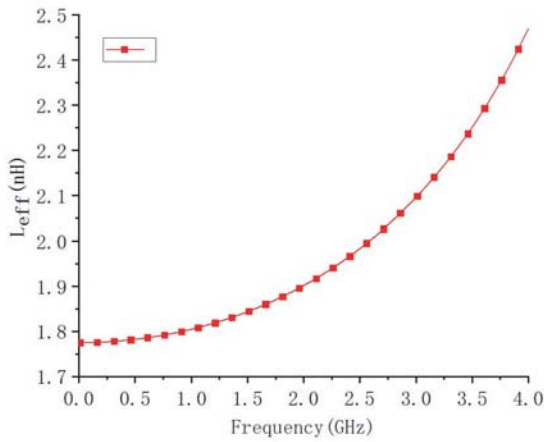


Figure 5. Effective inductance value of $L2$.

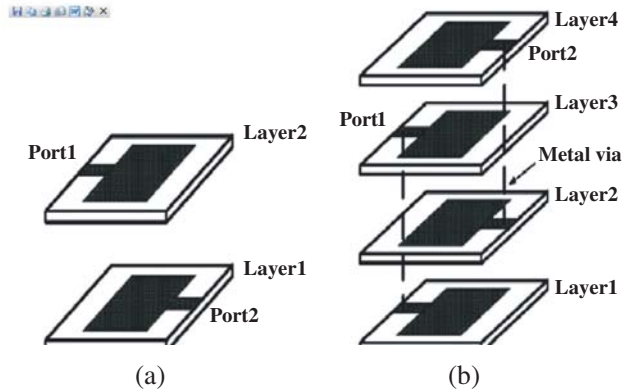


Figure 6. (a) MIM capacitor. (b) VIC capacitor.

resonance frequency. VIC structure uses more layers, which adds to the design difficulty and the process complexity. In an actual circuit design, it is necessary to make a choice between these two structures according to the structure and parameter values of the filter.

No matter which structure is chosen for the capacitor design, it is necessary to extract the relevant parameters of capacitor elements. Take the capacitor as a two-port network and extract its characteristic parameters, and then an accurate design of the structure and dimensions of the capacitor is obtained.

Regard to the capacitors in the filter, $C1 = 0.96 \text{ pF}$, $C3 = 0.81 \text{ pF}$, and their capacitance values are relatively small, so the embedded MIM structure is adopted. However, $C2 = 5 \text{ pF}$, and its capacitor value is relatively large. In order to reduce the plane area, an embedded VIC structure is adopted. The physical dimensions of $C1$, $C2$, and $C3$ are obtained through HFSS simulation, which is shown in Figure 7 and Figure 8. Compared with the traditional MIM structure, this structure has the advantages of small electrode area and high capacitor. The effective capacitor value is expressed by the scattering parameter as follows:

$$C_{eff} = -\frac{1}{2\pi f \times \text{im}(Z_{11})} \quad (5)$$

where C_{eff} is the effective value of capacitor, f the self-resonant frequency, and Z_{11} the impedance value of the capacitor. The VIC in Figure 7 is a three-layer capacitor structure with dimensions of $2.3 \text{ mm} \times 1.1 \text{ mm}$. The simulation results of the capacitor are as shown in Figure 8, and the effective capacitor value for 1.75 GHz is approximately 5 pF .

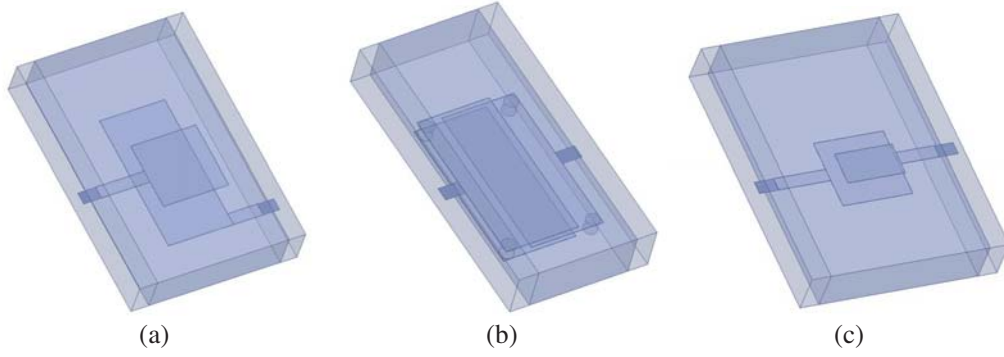


Figure 7. A three-dimensional model of LTCC capacitor (a) $C1$, (b) $C2$, (c) $C3$.

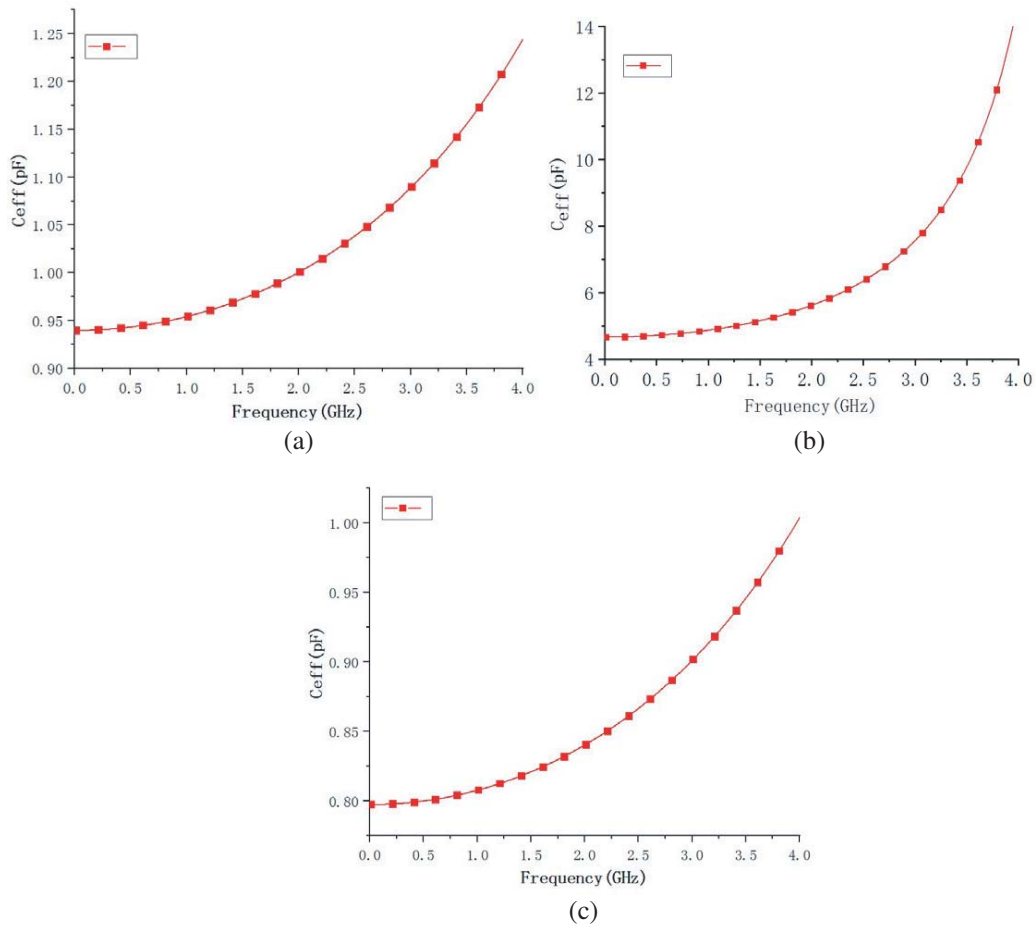


Figure 8. Effective inductance value (a) $C1$, (b) $C2$, (c) $C3$.

3.3. Establishing of Filter Structure and Simulation

Based on the models of inductors and capacitors, the three-dimensional modeling, simulation, and optimizing of all the components in the filter are performed. As shown in Figure 2, there are 5 inductors and 6 capacitors in total, and the values are different. The 11 variables have brought great difficulties in the processes of modeling and optimization. In order to facilitate the modeling and optimization, a symmetrical circuit structure is adopted in this paper. With the application of symmetry of the model, the 11 variables become 6 variables. Fewer variables in the schematic diagram gives ease in LTCC

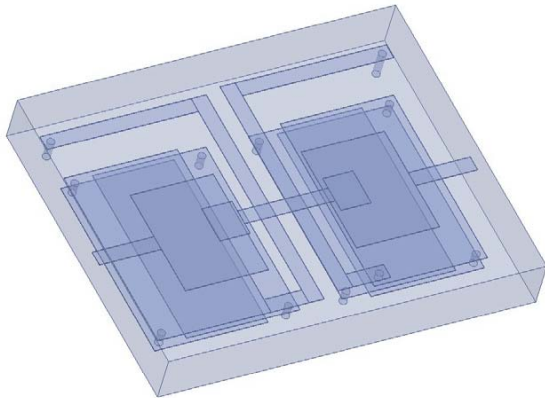


Figure 9. A three-dimensional model of the LTCC bandpass filter.

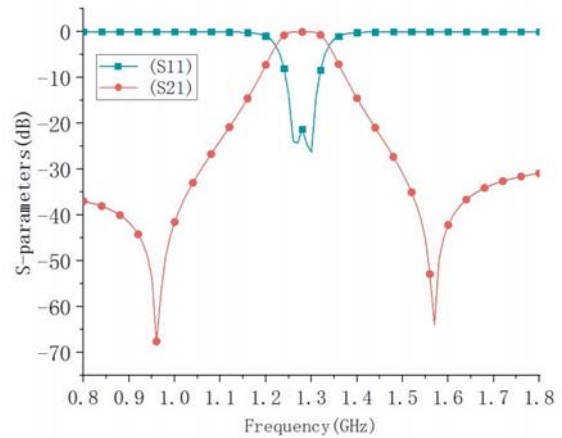


Figure 10. Simulation results of the LTCC bandpass filter.

integration. Since the simulation of this filter is difficult, optimization is done in the modeling process. The three-dimensional model of LTCC bandpass filter is shown in Figure 9.

By analyzing the simulation results of the flexible layout of the inductors and capacitors in model and constantly optimizing and adjusting the model, optimal simulation results are obtained as shown in Figure 10. From simulation results, it can be seen that within the bandwidth of 1.265 ~ 1.285 GHz, the insertion loss is relatively small, and the return loss is satisfactory. The out-of-band rejection also meets the requirements.

4. SIMULATION AND MEASUREMENT RESULTS

The production process of the LTCC is extremely complex, including punching via, filling, conductor printing, laminating, hot cutting, sintering, scribing, and post-burning. After these procedures, the production and processing of the LTCC filter is completed. The final product dimensions are only 5 mm × 4.1 mm × 1 mm. The actual processed L-band LTCC bandpass filter is shown in Figure 11. The test results are shown in Figure 12.

The simulation results of the filter with narrow-band and high out-of-band rejection are compared with the test results of actual products. The data of the two are roughly identical, and in particular, the two transmission zeros coincide with each other well with respect to the frequency position. The



Figure 11. Actual processed passband filter.

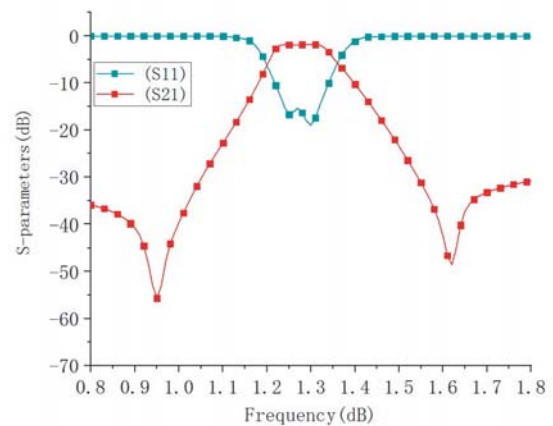


Figure 12. Test results.

insertion loss of the filter in the range of 1.265–1.285 GHz is less than 2 dB, and the VSWR is less than 1.5, which meets the requirements. As shown in Figure 12, the filter achieves better narrow-band characteristics. As transmission zeros are in good agreement with the simulation results, good out-of-band rejection is achieved. It can be seen from the test figure that the out-of-band rejection at 1 GHz is 39 dB, and that at 1.6 GHz is 42 dB, fully meeting the requirements.

The upper sideband roll-off rate of the filter simulation is 108.8 dB/GHz (attenuation: 3 dB at 1.22 GHz and 40 dB at 0.88 GHz). The lower sideband roll-off rate of the filter simulation is 185 dB/GHz (attenuation: 3 dB at 1.34 GHz and 40 dB at 1.54 GHz). The upper sideband roll-off rate of the filter measurement is 154.1 dB/GHz (attenuation: 3 dB at 1.22 GHz and 40 dB at 0.98 GHz). The lower sideband roll-off rate of the filter measurement is 142.3 dB/GHz (attenuation: 3 dB at 1.34 GHz and 40 dB at 1.6 GHz). Slight differences are shown between the results of the simulation and the results of the measurement. An analysis has been performed, and the possible causes have been found, which may be the uncertain factors during the manufacturing. The passband group delay results of the filter are as shown in Figure 13.

The simulated and measured insertion losses at the operating frequency band 1.265–1.285 GHz of the filter are as shown in Figure 14. The measured insertion loss varies from 1.8 to 2 dB, which is usable in communication applications.

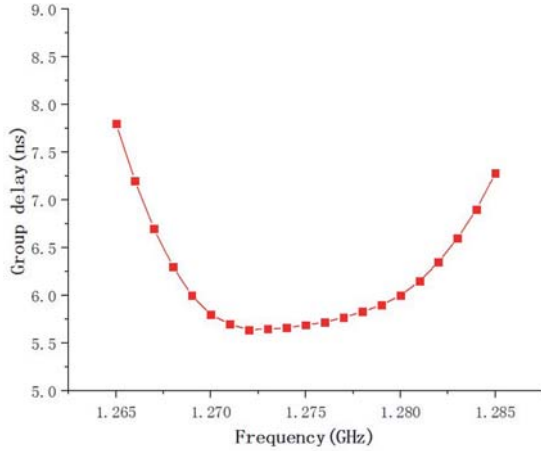


Figure 13. Passband group delay results of the filter.

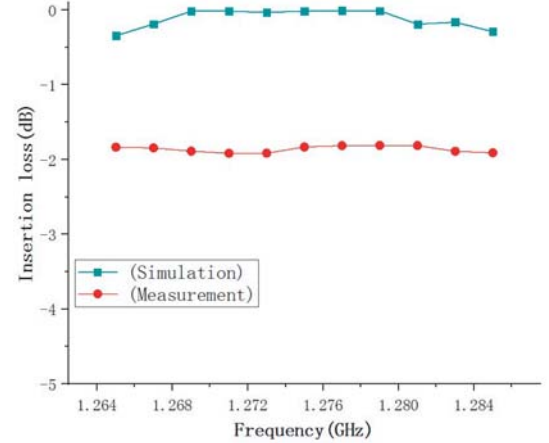


Figure 14. Insertion loss simulation and measurement results.

Table 2 shows the performance comparison between the proposed L-band bandpass filter and those of similar works in literature. The bandwidth of the proposed BPF is narrower than those in [19–22]. The proposed BPF has good insertion loss, better than those in [19–21] except [22]. The proposed BPF also has good return loss, better than those in [19, 20, 22] except [21]. The size of the proposed BPF is comparable to those in [20, 21] and more compact than [19] except [22].

Table 2. Comparison with similar works in literature.

| Ref. | f_c (GHz) | Bandwidth (MHz) | Insertion loss (dB) | Return loss (dB) | Size (mm) |
|------------------|--------------|-----------------|---------------------|------------------|---|
| [19] | 1.08 | 150 | 5.1 | 15 | $14 \times 6 \times 1.3$ |
| [20] | 1.46 | 250 | 2.56 | 15 | $4.5 \times 3.2 \times 1.5$ |
| [21] | 2.06 | 560 | 3.6 | 18 | $6.2 \times 2.1 \times 1$ |
| [22] | 2.45 | 100 | 1.55 | 15 | $1.6 \times 0.8 \times 0.7$ |
| This work | 1.275 | 20 | 2.0 | 16 | $5 \times 4.1 \times 1.0$ |

5. CONCLUSION

The design method of bandpass filter with narrow-band and high out-of-band rejection is introduced. This method is applied on the transmission zeros, and better out-of-band rejection is realized. With the idea of symmetry, the structure of filter can be simplified, and the difficulty in simulation can be reduced. As shown in test results, the simulated and measured results have good consistency. LTCC technology has big advantages in realizing miniaturization of the filter. Compared with a traditional crystal filter or SAW filter, the volume of an LTCC filter is at least five times smaller. At the same time, for the previous LTCC filter implementations, it is usually difficult to achieve narrow band. The design method in this paper provides a new idea for designing a narrow band bandpass filter.

REFERENCES

1. Mao, C., Y. Zhu, Z. Li, and X. Ming, "Design of LC bandpass filters based on silicon-based IPD technology," *2018 19th International Conference on Electronic Packaging Technology (ICEPT)*, 238–240, Shanghai, 2018.
2. Chen, J. and S. S. Liao, "Design of compact printed 2.4 GHz band-pass filter using LC resonator," *2016 International Conference on Advanced Materials for Science and Engineering (ICAMSE)*, 377–379, Tainan, 2016.
3. Xu, M., J. Tian, and P. Yang, "The design of LC resonator based bandpass filter embedded in LTCC substrate," *2009 2nd International Conference on Power Electronics and Intelligent Transportation System (PEITS)*, 301–305, Shenzhen, 2009.
4. Menicanin, A. B., M. S. Damnjanovic, L. D. Zivanov, and O. S. Aleksic, "Improved model of T-type LC EMI chip filters using new microstrip test fixture," *IEEE Transactions on Magnetics*, Vol. 47, No. 10, 3975–3978, Oct. 2011.
5. Cristal, E. G. and S. Frankel, "Hairpin-line and hybrid hairpin-line/half-wave parallel-coupled-line filters," *IEEE Transactions on Microwave Theory and Techniques*, Vol. 20, No. 11, 719–728, Nov. 1972.
6. Chang, C.-Y., C.-C. Chen, and H.-J. Huang, "Folded quarter-wave resonator filters with Chebyshev, flat group delay, or quasi-elliptical function response," *2002 IEEE MTT-S Int. Microw. Symp. Dig. (Cat. No.02CH37278)*, Vol. 3, 1609–1612, Seattle, WA, USA, 2002.
7. Huang, F., "Ultra-compact superconducting narrow-band filters using single- and twin-spiral resonators," *IEEE Transactions on Microwave Theory and Techniques*, Vol. 51, No. 2, 487–491, Feb. 2003.
8. Zhang, Yu., K. A. Zaki, A. J. Piloto, and J. Tallo, "Miniature broadband bandpass filters using double-layer coupled stripline resonators," *IEEE Transactions on Microwave Theory and Techniques*, Vol. 54, No. 8, 3370–3377, Aug. 2006.
9. Yeung, L. K. and K.-L. Wu, "A compact second-order LTCC bandpass filter with two finite transmission zeros," *IEEE Transactions on Microwave Theory and Techniques*, Vol. 51, No. 2, 337–341, Feb. 2003.
10. Yang, F., R.-Z. Liu, H.-X. Yu, X.-Y. He, and Y. Zhou, "Miniaturized folded substrate integrated waveguide filters in LTCC," *2011 IEEE International Conference on Microwave Technology & Computational Electromagnetics*, 171–173, Beijing, 2011.
11. Feng, W., X. Gao, W. Che, and W. Yang, "High performance LTCC wideband bandpass filter based on coupled lines," *2017 IEEE MTT-S International Microwave Workshop Series on Advanced Materials and Processes for RF and THz Applications (IMWS-AMP)*, 1–3, Pavia, 2017.
12. Wang, S. and P. Wang, "The design of a compact LTCC balanced filter for Bluetooth applications," *2012 International Conference on Computational Problem-Solving (ICCP)*, 267–270, Leshan, 2012.
13. Saad, M. R., et al., "Designing 5 GHz microstrip coupled line bandpass filter using LTCC technology," *2008 International Conference on Electronic Design*, 1–4, Penang, 2008.
14. Sheen, J. W., "A compact semi-lumped low-pass filter for harmonics and spurious suppression," *IEEE Microwave and Guided Wave Letters*, Vol. 10, No. 3, 92–93, Mar. 2000.

15. Dai, Y., L. Xu, Q. Han, S. Chen, L. Wang, and R. Chen, "Miniaturized LTCC wideband bandpass filter using lumped-element shunt LC resonators," *2012 International Conference on Microwave and Millimeter Wave Technology (ICMMT)*, 1–3, Shenzhen, 2012.
16. Cui, L., J. Yu, S. Li, and Y. Liu, "A sharp-rejection dual-bandstop filter with multiple transmission poles and zeros based on transversal signal-interaction concepts," *2017 IEEE 5th International Symposium on Electromagnetic Compatibility (EMC-Beijing)*, 1–4, Beijing, 2017.
17. Dai, Y.-S., et al., "LTCC bandpass filter for BluetoothTM application with dual transmission zeros," *2008 International Conference on Microwave and Millimeter Wave Technology*, 284–286, Nanjing, 2008.
18. Matthaei, G. L., L. Young, and E. M. T. Jones, *Microwave Filter, Impedance-matching Networks, and Coupling Structures*, Chap. 8, McGraw-Hill, New York, 1964.
19. Wang, Z., Y. Tian, S. Bu, and Z. Luo, "Study of L-band miniature lumped element LTCC band-pass filter," *2010 International Conference on Microwave and Millimeter Wave Technology*, 864–866, Chengdu, 2010, doi: 10.1109/ICMMT.2010.5525175.
20. Sun, C., Y. Dai, and B. Li, "Design of four-order distributed band-pass filter based on LTCC technology," *2016 IEEE MTT-S International Microwave Workshop Series on Advanced Materials and Processes for RF and THz Applications (IMWS-AMP)*, 1–3, Chengdu, 2016, doi: 10.1109/IMWS-AMP.2016.7588436.
21. Li, B. and Y. Dai, "High performance five-order band-pass filter based on LTCC technology research," *2016 IEEE International Workshop on Electromagnetics: Applications and Student Innovation Competition (iWEM)*, 1–3, Nanjing, 2016, doi: 10.1109/iWEM.2016.7504880.
22. Chen, L. and K. Lin, "A minimized dual-band bandpass filter using series $\lambda/4$ resonators and open stub line," *2016 IEEE 5th Asia-Pacific Conference on Antennas and Propagation (APCAP)*, 159–160, Kaohsiung, 2016, doi: 10.1109/APCAP.2016.7843147.